



HAL
open science

Multiscale modeling of crystalline nanostructures

Julien Yvonnet, A. Mitrushchenkov, Gilberte Chambaud, Qi-Chang He

► **To cite this version:**

Julien Yvonnet, A. Mitrushchenkov, Gilberte Chambaud, Qi-Chang He. Multiscale modeling of crystalline nanostructures. 10e colloque national en calcul des structures, May 2011, Giens, France. pp.Clé USB. hal-00592702

HAL Id: hal-00592702

<https://hal.science/hal-00592702>

Submitted on 3 May 2011

HAL is a multi-disciplinary open access archive for the deposit and dissemination of scientific research documents, whether they are published or not. The documents may come from teaching and research institutions in France or abroad, or from public or private research centers.

L'archive ouverte pluridisciplinaire **HAL**, est destinée au dépôt et à la diffusion de documents scientifiques de niveau recherche, publiés ou non, émanant des établissements d'enseignement et de recherche français ou étrangers, des laboratoires publics ou privés.

A multiscale method for modeling size and surface effects in crystalline nanowires based on finite element and quantum mechanics

J. Yvonnet¹, A. Mitrushchenkov¹, G. Chambaud¹, Q.-C. He¹

¹ MSME, Université Paris-Est, France, {julien.yvonnet, Alexander.Mitrushchenkov, Gilberte.Chambaud, Qi-Chang.He}@univ-paris-est.fr

Résumé — A multiscale procedure for modeling crystalline nanostructures such as nanowires is proposed. The size effects exhibited by nano objects are captured by taking into account a surface energy, following the classical Gurtin Murdoch surface elasticity theory. An appropriate variational form and a finite element approach are provided to model and solve relevant problems numerically. The methodology is completed with a computational procedure based on *ab initio* calculations to extract elastic coefficients of general anisotropic surfaces.

Mots clés — Nanomechanics, Surface effects, Multiscale methods.

1 Introduction

Nanosized objects have at least one dimension in the nanometer range, roughly between 1 to 100 nm. They are intermediate in size between atomistic/molecular and microscopic/continuum structures. By assembling nanostructural elements, it is possible to manufacture nanocomposites or nanodevices with desired properties and functions. Various types of nanostructural elements like nanowires, nanotubes, nanorods, nanorings, nanobelts or nanocombs have been synthesized and can serve as building blocks for nanosystems and nanostructures.

Nanowires and in general nanostructures are characterized by non zero surface energy that make their effective properties size-dependent. Due to a different local environment, atoms near a free surface or interface have different equilibrium positions than do atoms in the bulk.

Surface free energy is neglected in traditional continuum mechanics because it is associated with only a few layers of atoms. For objects with dimensions larger than tens of nanometers, the ratio between volume and surface is extremely small. However, for nano-sizes particles, wires and films, this ratio becomes significant, and so does the effect of surface free energy. The importance of surface stress has led to important theoretical modeling advances that has started with the works of Gurtin and Murdoch [4].

This work provides a complete procedure for modeling size-dependent mechanical effects in nanowires. Firstly, a continuum variational framework enriched with surface energy is developed, and a three-dimensional FEM methodology is presented to solve the problem numerically. Secondly, a new technique based on *ab initio* computations is detailed to determine the surface parameters related to the continuum model.

2 Continuum modelling with surface energy

We consider an open domain $\Omega \in \mathbb{R}^3$ with a bounding surface Γ . The latter Γ is composed of two disjoint complementary parts Γ_u and Γ_F where the displacements and forces are prescribed, respectively. To introduce the surface energy and related size effects, the Gurtin-Murdoch model [4] of surface elasticity is adopted. The equilibrium equations of the problem are then given by

$$\nabla \cdot \boldsymbol{\sigma} + \mathbf{b} = 0 \text{ in } \Omega, \quad (1)$$

$$\nabla^s \cdot \boldsymbol{\sigma}^s + \boldsymbol{\sigma} \mathbf{n} = 0 \text{ on } \Gamma \quad (2)$$

where $\boldsymbol{\sigma}$ is the Cauchy stress tensor, \mathbf{b} is body force and \mathbf{n} is the outward unit normal vector to Γ . Equation (1) refers to the bulk equilibrium equation, while Eq. (2) refers to the surface equilibrium (see e.g. [1]). Superscript $(\cdot)^s$ refers to surface quantities or operators. In Eq. (2), $\nabla^s \cdot \mathbf{T}$ denotes the surface divergence of a differentiable second-order tensor \mathbf{T} and is defined by :

$$\nabla^s \cdot \mathbf{T} = \nabla \mathbf{T} : \mathbf{P}. \quad (3)$$

In the above equation, the symbol $:$ denotes double contraction of indices and $\mathbf{P}(\mathbf{x}) = \mathbf{1} - \mathbf{n}(\mathbf{x}) \otimes \mathbf{n}(\mathbf{x})$ is an orthogonal projection operator describing the projection on the plane tangent to Γ at $\mathbf{x} \in \Gamma$. The surface strain and stress tensors are defined by :

$$\boldsymbol{\sigma}^s = \mathbf{P} \boldsymbol{\sigma} \mathbf{P}, \quad \boldsymbol{\varepsilon}^s = \mathbf{P} \boldsymbol{\varepsilon} \mathbf{P}, \quad (4)$$

where $\boldsymbol{\varepsilon} = \frac{1}{2}(\nabla \mathbf{u} + \nabla \mathbf{u}^T)$ is the linearized strain tensor and \mathbf{u} is a displacement field. It is worth noting that the operator \mathbf{P} does not involve any basis change : the reader has to keep in mind that \mathbf{T}^s denotes the projection of \mathbf{T} on the surface Γ . Thus $\mathbf{T}^s = \mathbf{P} \mathbf{T} \mathbf{P}$ does not express the components relative to the basis of the tangent plane to the surface. This projection tensor nicely allows one to mix bulk and surface quantities in one equation. The surface stress $\boldsymbol{\sigma}^s$ is related to the surface strain by

$$\boldsymbol{\sigma}^s = \frac{\partial \gamma_0^s(\boldsymbol{\varepsilon}^s)}{\partial \boldsymbol{\varepsilon}^s} + \frac{\partial \gamma^s(\boldsymbol{\varepsilon}^s)}{\partial \boldsymbol{\varepsilon}^s}. \quad (5)$$

Above, $\gamma_0^s(\boldsymbol{\varepsilon}_0^s)$ and $\gamma^s(\boldsymbol{\varepsilon}^s)$ are specified by

$$\gamma_0^s(\boldsymbol{\varepsilon}^s) = \boldsymbol{\tau}^s : \boldsymbol{\varepsilon}^s, \quad \gamma^s(\boldsymbol{\varepsilon}^s) = \frac{1}{2} \boldsymbol{\varepsilon}^s : \mathbb{C}^s : \boldsymbol{\varepsilon}^s. \quad (6)$$

Physically, $\gamma_0^s(\boldsymbol{\varepsilon}^s)$ is an energy density due to surface residual stress $\boldsymbol{\tau}^s$, $\gamma^s(\boldsymbol{\varepsilon}^s)$ is a surface strain density function with \mathbb{C}^s denoting a surface elastic tensor. We do not assume an isotropic surface, i.e. $\boldsymbol{\tau}^s \neq \boldsymbol{\tau}^s \mathbf{P}$. The equations (1-2) are completed with boundary conditions prescribed on the surface Γ_u and Γ_F as

$$\begin{cases} \boldsymbol{\sigma} \mathbf{n} = \bar{\mathbf{F}} & \text{on } \Gamma_F \\ \mathbf{u}(\mathbf{x}) = \bar{\mathbf{u}}(\mathbf{x}) & \text{on } \Gamma_u. \end{cases} \quad (7)$$

Finally, it is assumed that the surface adheres to the bulk :

$$[[\mathbf{u}]] = 0 \text{ on } \Gamma. \quad (8)$$

To apply this framework to finite element analysis, we provide in the following the weak form of the equations. It can be derived straightforwardly by taking the classical weak form and taking into account a term related to the virtual internal work of the surface [7]. Another way to obtain it is to express the potential energy of the system and minimize the energy with respect to the displacement field. Thus, the potential energy of the system is given by :

$$E = W^b(\boldsymbol{\varepsilon}) + W^s(\boldsymbol{\varepsilon}^s) - W^{ext}. \quad (9)$$

In the above expression, $W^b(\boldsymbol{\varepsilon})$ is the bulk elastic strain energy given by

$$W^b(\boldsymbol{\varepsilon}) = \int_{\Omega} \frac{1}{2} \boldsymbol{\varepsilon} : \mathbb{C}^{bulk} : \boldsymbol{\varepsilon} d\Omega. \quad (10)$$

In (9), $W^s(\boldsymbol{\varepsilon}^s)$ is the surface elastic energy provided by

$$W^s(\boldsymbol{\varepsilon}^s) = \int_{\Gamma} [\gamma_0^s(\boldsymbol{\varepsilon}^s) + \gamma^s(\boldsymbol{\varepsilon}^s)] d\Gamma. \quad (11)$$

Finally, the work of external forces is expressed by :

$$W^{ext} = \int_{\Gamma_F} \mathbf{u} \cdot \bar{\mathbf{F}} d\Gamma + \int_{\Omega} \mathbf{u} \cdot \mathbf{b} d\Omega. \quad (12)$$

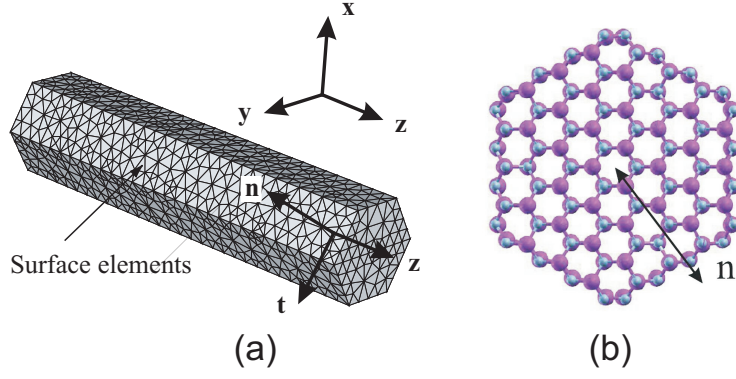


FIGURE 1 – (a) Local basis and FEM model of nanowire with hexagonal cross-section; (b) ab initio model of nanowire with n layers.

The equilibrium is found by writing the stationarity condition :

$$D_{\delta \mathbf{u}} E = 0 \quad (13)$$

where $D_{\mathbf{v}} f$ is the Gâteaux derivative of the functional f in the direction \mathbf{v} . It leads to the weak form suitable for finite element discretization :

Find $\mathbf{u} \in H^1(\Omega)$ and $\mathbf{u} = \bar{\mathbf{u}}$ on Γ_u such as

$$\begin{aligned} & \int_{\Omega} \boldsymbol{\varepsilon}(\mathbf{u}) : \mathbb{C}^{bulk} : \boldsymbol{\varepsilon}(\delta \mathbf{u}) d\Omega + \int_{\Gamma} \boldsymbol{\varepsilon}^s(\mathbf{u}) : \mathbb{C}^s : \boldsymbol{\varepsilon}^s(\delta \mathbf{u}) d\Gamma \\ & = \int_{\Gamma_F} \bar{\mathbf{F}} \cdot \delta \mathbf{u} d\Gamma + \int_{\Omega} \mathbf{b} \cdot \delta \mathbf{u} d\Omega - \int_{\Gamma} \boldsymbol{\tau}^s : \delta \boldsymbol{\varepsilon}^s(\delta \mathbf{u}) d\Gamma \end{aligned} \quad (14)$$

for all $\delta \mathbf{u} \in H_0^1(\Omega)$, $H^1(\Omega)$ and $H_0^1(\Omega)$ being the usual Sobolev spaces.

2.0.1 Discretization with finite elements

In the following the Voigt's notation is adopted. The vectorial form of the stress tensor is given by $[\boldsymbol{\sigma}] = \{\sigma_{11}, \sigma_{22}, \sigma_{33}, \sigma_{23}, \sigma_{13}, \sigma_{12}\} = \{\sigma_1, \sigma_2, \sigma_3, \sigma_4, \sigma_5, \sigma_6\}$ and the strain tensor counterpart is given by $[\boldsymbol{\varepsilon}] = \{\varepsilon_{11}, \varepsilon_{22}, \varepsilon_{33}, 2\varepsilon_{23}, 2\varepsilon_{13}, 2\varepsilon_{12}\} = \{\varepsilon_1, \varepsilon_2, \varepsilon_3, \varepsilon_4, \varepsilon_5, \varepsilon_6\}$. The indices 1, 2 and 3 correspond to the \mathbf{x} , \mathbf{y} and \mathbf{z} directions, respectively (see figure 1). In this work we consider the nanowire which is a monocrystal with wurtzite structure, as for example AlN, which grows with hexagonal cross-sections (see figure 1) and whose bulk elastic tensor can be expressed by 5 independent constants $C_{11}, C_{33}, C_{44}, C_{12}$ and C_{13} .

To solve the problem by FEM, it is necessary to discretize the weak form (14). While the bulk terms lead to classical matrix and vector forms, terms related to surface energy require a specific treatment. The domain is first discretized into volume elements, as shown in figure 1.

To discretize the surface terms, surface elements are required. In [7], we proposed a framework avoiding the explicit mesh of surfaces when considering surface energy by using an XFEM/level-set approach. In this work however, we adopt the classical FEM framework for the sake of simplicity. Let $(\mathbf{e}_1, \mathbf{e}_2)$ a local orthonormal basis related to the surface such that $\mathbf{e}_1 = \mathbf{t}$ and $\mathbf{e}_2 = \mathbf{z}$, with \mathbf{z} and $\mathbf{t} = \mathbf{z} \times \mathbf{n}$ unit vectors along the main direction of the nanowire and tangent to the surface Γ (see figure 1).

The surface residual stress can be expressed by :

$$\boldsymbol{\tau}^s = \tau_1^s \mathbf{e}_1 \otimes \mathbf{e}_1 + \tau_3^s \mathbf{e}_2 \otimes \mathbf{e}_2 = \tau_1^s \mathbf{t} \otimes \mathbf{t} + \tau_3^s \mathbf{z} \otimes \mathbf{z}. \quad (15)$$

Due to the symmetry of the hexagonal nanowire, the six facets are identical and correspond to the $(10\bar{1}0)$ surfaces. Then the surface stress can be related to surface strain through four independent constants $C_{11}^s, C_{13}^s, C_{33}^s$ and C_{55}^s and two residual stress components τ_1^s and τ_3^s :

$$\begin{bmatrix} \sigma_1^s \\ \sigma_3^s \\ \sigma_5^s \end{bmatrix} = \begin{bmatrix} C_{11}^s & C_{13}^s & 0 \\ C_{13}^s & C_{33}^s & 0 \\ 0 & 0 & C_{55}^s \end{bmatrix} \begin{bmatrix} \varepsilon_1^s \\ \varepsilon_3^s \\ 2\varepsilon_5^s \end{bmatrix} + \begin{bmatrix} \tau_1^s \\ \tau_3^s \\ 0 \end{bmatrix}. \quad (16)$$

The elastic tensor is expressed in the local basis as :

$$\begin{aligned} \mathbb{C}^s = & C_{11}^s \mathbf{t} \otimes \mathbf{t} \otimes \mathbf{t} \otimes \mathbf{t} + C_{33}^s \mathbf{z} \otimes \mathbf{z} \otimes \mathbf{z} \otimes \mathbf{z} \\ & + C_{13}^s (\mathbf{t} \otimes \mathbf{t} \otimes \mathbf{z} \otimes \mathbf{z} + \mathbf{z} \otimes \mathbf{z} \otimes \mathbf{t} \otimes \mathbf{t}) + C_{55}^s (\mathbf{t} \otimes \mathbf{z} \otimes \mathbf{t} \otimes \mathbf{z} + \mathbf{z} \otimes \mathbf{t} \otimes \mathbf{z} \otimes \mathbf{t}). \end{aligned} \quad (17)$$

On substituting the FEM discretization into the weak form (14), and using the arbitrariness of nodal variations $\delta \mathbf{u}$, the following discrete system of linear equations is obtained :

$$(\mathbf{K} + \mathbf{K}^s) \mathbf{q} = \mathbf{F} - \mathbf{F}^s \quad (18)$$

with \mathbf{q} being the vector of unknown displacements,

$$\mathbf{K} = \int_{\Omega} \mathbf{B}^T \mathbf{C}^{bulk} \mathbf{B} d\Omega \quad (19)$$

being the bulk rigidity matrix and

$$\mathbf{K}^s = \int_{\Gamma} \mathbf{B}^T \mathbf{M}_p^T \mathbf{C}^s \mathbf{M}_p \mathbf{B} d\Gamma \quad (20)$$

being the surface rigidity matrix. In (20) \mathbf{C}^s is the matrix form of the tensor (17) such as $[\boldsymbol{\sigma}^s] = \mathbf{C}^s [\boldsymbol{\varepsilon}^s]$, with $[\boldsymbol{\sigma}^s] = \{\sigma_{11}^s, \sigma_{22}^s, \sigma_{33}^s, \sigma_{23}^s, \sigma_{13}^s, \sigma_{12}^s\}$ and $[\boldsymbol{\varepsilon}^s] = \{\varepsilon_{11}^s, \varepsilon_{22}^s, \varepsilon_{33}^s, 2\varepsilon_{23}^s, 2\varepsilon_{13}^s, 2\varepsilon_{12}^s\}$. Note that $[\boldsymbol{\sigma}^s]$ is different from the left-hand term in (16) which express the surface stress in the local basis (tangent to the surface) while $[\boldsymbol{\sigma}^s]$ is expressed in the cartesian basis. As \mathbf{C}^s is symmetric (see Eq. (17)), the matrix \mathbf{K}^s is also symmetric. The matrix \mathbf{M}_p relates the surface strains to the bulk strains through $[\boldsymbol{\varepsilon}^s] = \mathbf{M}_p [\boldsymbol{\varepsilon}]$. Its expression in 3D is specified by

$$\mathbf{M}_p = \begin{bmatrix} P_{11}^2 & P_{12}^2 & P_{13}^2 \\ P_{12}^2 & P_{22}^2 & P_{23}^2 \\ P_{13}^2 & P_{23}^2 & P_{33}^2 \\ 2P_{12}P_{13} & 2P_{22}P_{23} & 2P_{23}P_{33} \\ 2P_{11}P_{13} & 2P_{12}P_{23} & 2P_{13}P_{33} \\ 2P_{11}P_{12} & 2P_{12}P_{22} & 2P_{13}P_{23} \\ P_{12}P_{13} & P_{11}P_{13} & P_{11}P_{12} \\ P_{22}P_{23} & P_{12}P_{23} & P_{12}P_{22} \\ P_{23}P_{33} & P_{13}P_{33} & P_{13}P_{23} \\ (P_{23}^2 + P_{22}P_{33}) & (P_{23}P_{13} + P_{12}P_{33}) & (P_{22}P_{13} + P_{12}P_{23}) \\ (P_{13}P_{23} + P_{12}P_{33}) & (P_{13}^2 + P_{11}P_{33}) & (P_{12}P_{13} + P_{11}P_{23}) \\ (P_{13}P_{22} + P_{12}P_{23}) & (P_{11}P_{23} + P_{13}P_{12}) & (P_{11}P_{22} + P_{12}^2) \end{bmatrix}. \quad (21)$$

We finally obtain the following approximation for \mathbf{K}^s :

$$\mathbf{K}^s \simeq \sum_{e \in \mathcal{S}^{\Gamma}} \mathbf{B}^T(\mathbf{x}_{\Omega}^e) \mathbf{M}_p^T(\mathbf{x}_{\Gamma}^e) \mathbf{C}^s(\mathbf{x}_{\Gamma}^e) \mathbf{M}_p(\mathbf{x}_{\Gamma}^e) \mathbf{B}(\mathbf{x}_{\Omega}^e) |\Gamma^e| \quad (22)$$

where $|\Gamma^e|$ denotes the area of the triangular element Γ^e , \mathbf{x}_{Ω}^e is an integration point in the element and \mathbf{x}_{Γ}^e is an integration point on the external surface of the element (see more details in [8]). Remark that integration points being located inside triangular facets, the unit normal vector \mathbf{n} and tangent projector \mathbf{P} are well defined. In this work we exclude the surface energies of both ends surfaces where displacement and external forces are prescribed. The generalized force vectors are obtained by

$$\mathbf{F} = \int_{\Gamma_F} \mathbf{N}^T \bar{\mathbf{F}} d\Gamma + \int_{\Omega} \mathbf{N}^T \mathbf{b} d\Omega \quad (23)$$

$$\mathbf{F}^s = \int_{\Gamma} \mathbf{B}^T \mathbf{M}_p^T \boldsymbol{\tau}^s d\Gamma, \quad (24)$$

where \mathbf{N} is a classical FEM shape functions matrix. In the following, body forces are neglected.

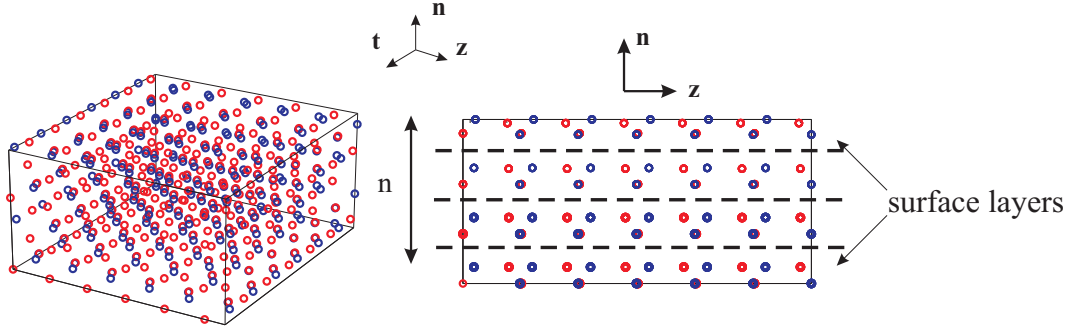


FIGURE 2 – Slab models with number of layers n .

3 Extracting coefficients using Quantum Mechanics calculations

In the present work, bulk and surface elastic parameters are extracted through atomistic *ab initio* calculations. In the present work we used the CRYSTAL code [2] for all *ab initio* calculations. B3LYP KS-DFT method with extra large space integration grid, was used. Basis set was 86-21G* for Al [6], and 6-31Gd1G for N[3]. We have chosen the hybrid B3LYP functional because it is known to provide quite accurate energetic properties. As we are interested in elastic behavior, which is evaluated through energy derivatives, this choice seems appropriate.

3.1 Surface coefficients

To compute surface elastic parameters, a surface (slab) model shown in figure 2 is used, consisting of n layers of atoms in the direction normal to the surface. Periodic conditions are applied along both other directions.

The possible strains for the slab system are ϵ_1^s , ϵ_3^s and ϵ_5^s which are prescribed along the z -(3) and t -(1) directions. The upper and lower surfaces normal to \mathbf{n} are free to relax. The total energy of the system is the sum of two components, the surface energy and the bulk energy. The surface energy has to be isolated from the total energy. We assume the following model :

$$E^{slab}(w) = wE^s + (1-w)E^{slab}(w \rightarrow 0) \quad , \quad w = \frac{2}{n} \quad (25)$$

where w is the relative weight of the surface for a n -layer slab, as the model depicted in figure 2 contains two external atomic layers. Defining the elastic constants as derivatives of the energy with respect to strains, we obtain

$$C_{ij}^{slab}(w) = wC_{ij}^s + (1-w)C_{ij}^{slab}(w \rightarrow 0) \quad (26)$$

where C_{ij}^s are the surface elastic properties and $C_{ij}^{slab}(w \rightarrow 0)$ are the limit values which can be obtained from bulk term by fully relaxing ϵ_2 for fixed ϵ_1 and ϵ_3 and optimizing the energy of the system.

Eq. (26) can be re-arranged as

$$C_{ij}(w) = w(C_{ij}^s - C_{ij}^{slab}(w \rightarrow 0)) + C_{ij}^{slab}(w \rightarrow 0). \quad (27)$$

The procedure consists into computing values of C_{ij} for different values of w (by increasing the number of layers n) and fitting the obtained curve with a linear function to identify the slope $r = C_{ij}^s - C_{ij}^{slab}(w \rightarrow 0)$ and thus C_{ij}^s . For the residual stress we have :

$$\tau_i(w) = w\tau_i^s. \quad (28)$$

In that case τ_i^s are directly obtained from the slope of the linear fit (see an illustration in [5]). We define per-area elastic constants as

$$C_{ij}^{slab} = \frac{1}{S} \frac{\partial^2 E^{slab}}{\partial \epsilon_i \partial \epsilon_j} \quad (29)$$

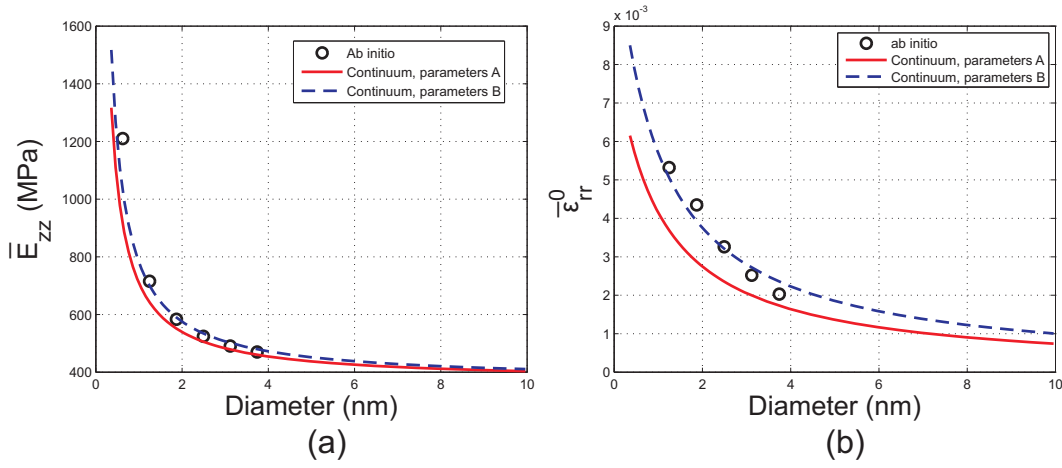


FIGURE 3 – (a) Effective Young modulus of the nanowire : comparison between continuum FEM model and *ab initio* model (prescribed stress) ; (b) Nanowire Bulk radial strain in relaxation : comparison between continuum FEM model and *ab initio* model

where $S = ac$ is the unit cell area. The total surface energy E^{slab} is determined using the DFT method described above for several values of strains ϵ_1 , ϵ_2 and ϵ_5 . As for bulk computations, a polynomial fitting was used to extract the derivatives. The resulting surface parameters were provided for the (10 $\bar{1}$ 0) AlN wurtzite surfaces in [5, 8] (parameters A).

4 Numerical examples

4.1 Validation of the model : nanowire in traction

The aim of this first example is to validate the mechanical continuum model by comparing it with *ab initio* calculations. Different atomistic models fully solved with an *ab initio* method are constructed with increasing diameters. We classify the nanowires according to the number of atomic layers n in the nanowires (see figure 1 b). The biggest calculated nanowire corresponds to $n = 7$ and contains 588 atoms in the unit cell. As both periodic conditions along z-axis and hexagonal symmetries are taken into account, a reduced model containing 98 atoms is employed.

We compute two quantities for both models : the Young modulus \bar{E}_{zz} and the axial strain of the nanowire in absence of loading due to surface residual stress τ^s and (c) the bulk radial residual strain ϵ_{rr}^0 (see more results in [8]).

Results are presented in figures 3 (a)-(b). A mesh containing 8905 nodes was used to plot the continuous curves.

We can observe from figure 3 that the agreement between the continuum and *ab initio* models is good in regards to Young's modulus and axial relaxation strain, when employing the coefficients obtained from the slab procedure without any modification. The use of optimized coefficients [8] gives rise to a slight improvement.

From the above results, we conclude that the model has a good accuracy regarding the effective properties of the nanowire. In what follows, we examine the local fields. A continuous displacement field is constructed from the *ab initio* discrete atomic displacements.

We can notice from figure 4 that in the bulk region both displacement fields are in very good agreement, especially when the set of optimized surface coefficients B is used. However, near the surface, the local fields are poorly reproduced. This can be partly explained by the fact that both Al and N atoms have very different kinematics [8]. On the surface layer, Al atoms possess a relatively large inward radial displacement as compared to the Al atoms in the next interior layer and with opposite sign to the N atoms which have an outward displacement on the surface. This highly heterogeneous field cannot be captured accurately by the proposed continuum model.

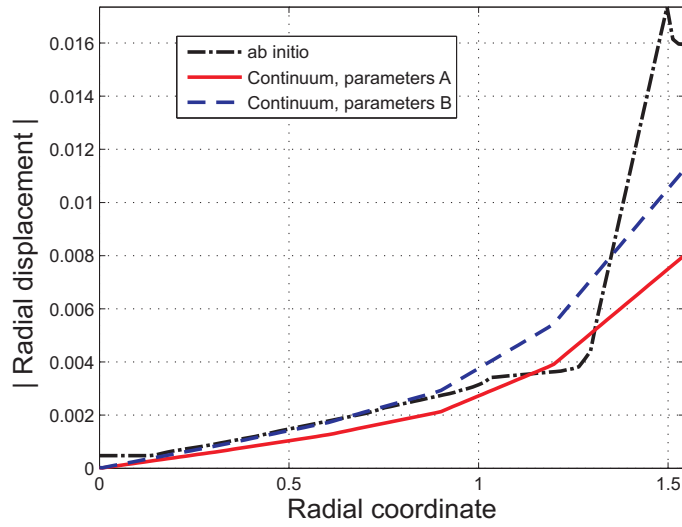


FIGURE 4 – Radial displacement field along nanowire radial direction ($d = 3.11$ nm). Comparison between continuum model and *ab initio* interpolated atomic displacements.

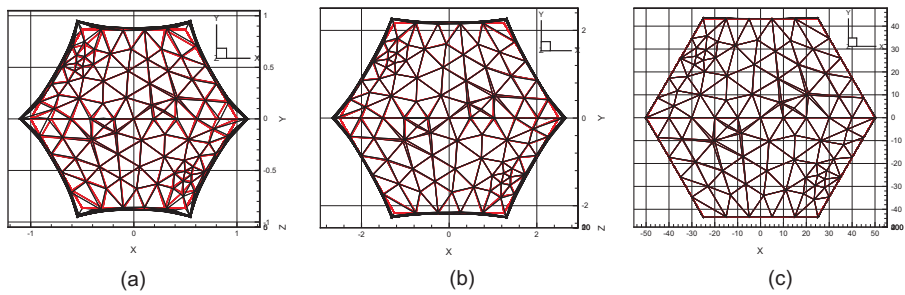


FIGURE 5 – Deformed configuration of the nanowire in free relaxation (magnified 10 times) for (a) $d = 2$ nm; (b) $d = 5$ nm; (c) $d = 100$ nm. Red and black meshes correspond to undeformed and deformed configuration, respectively.

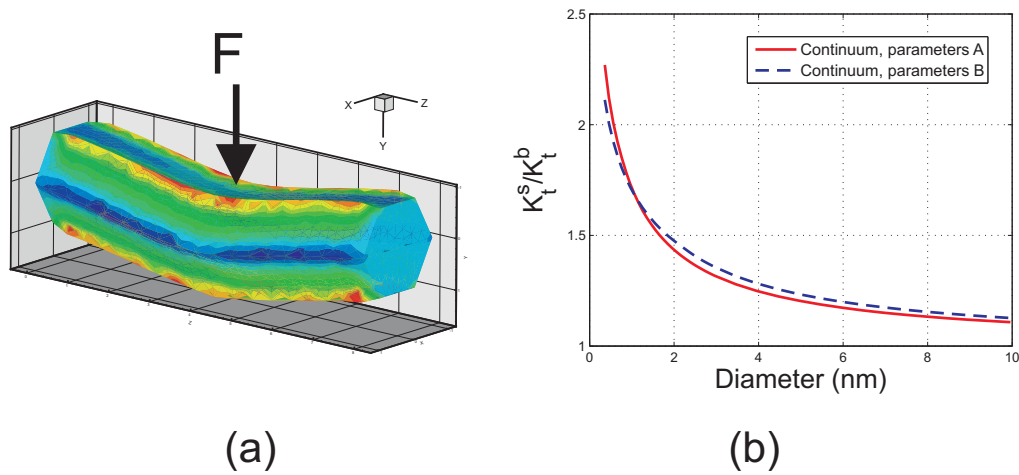


FIGURE 6 – (a) ϵ_{yy} strain field and deformed configuration of the nanowire in bending ; (b) Transverse stiffness of the nanowire versus diameter.

4.2 Bending of a nanowire

In this example, the constructed continuum model is employed to study size effects in bending analysis of a nanowire. This problem is not tractable via *ab initio* calculations, as no periodicity can be considered. This test is of practical importance, as this type of loading can be prescribed for example using an atomic force microscope (AFM). The nanowire is clamped at its both ends and subjected to a force distribution $\mathbf{F} = \sigma_y \mathbf{e}_y \otimes \mathbf{e}_y \mathbf{n}$, $\sigma_y = 1e - 8$ MPa on a width $l = L/20$. As in previous example, the length of the nanowire is taken as $L = 4d$.

To evaluate the influence of surface effects, we compute the transverse stiffness as a function of the nanowire diameter. The results are presented in figure 6. The size effects can be clearly observed.

Références

- [1] T. Chen, M.-S. Chiu, C.-N. Weng. *FDerivation of the generalized Young-Laplace equation of curved interfaces in nanoscaled solids*, J. Appl. Phys., 100 :074308, 2006.
- [2] R. Dovesi, V.R. Saunders, C. Roetti, R. Orlando, C. M. Zicovich-Wilson, F. Pascale, B. Civalleri, K. Doll, N.M. Harrison, I.J. Bush, Ph. D'Arco, M. Llunell. *CRYSTAL06 User's Manual*, University of Torino, Torino, 2006.
- [3] C. Gatti, V.R. Saunders, C. Roetti. *Crystal-field effects on the topological properties of the electron-density in molecular-crystals - the case of urea*, J. Chem. Phys., 101, 10686-10696, 1994.
- [4] M.E. Gurtin, A.I. Murdoch. *Continuum theory of elastic-material surfaces*, Arch. Ration. Mech. Anal., 57(4), 291-323, 1975.
- [5] A. Mitrushchenkov, G. Chambaud, J. Yvonnet, Q.-C. He. *Towards an elastic model of wurtzite AlN model*, Nanotechnology, 21(25), 255702, 2010.
- [6] B. Montanari, B. Civalleri, C.M. Zicovich-Wilson, R. Dovesi. *Influence of the exchange-correlation functional in all-electron calculations of the vibrational frequencies of corundum (alpha-Al₂O₃)*, Int. J. Quantum Chem., 106, 1703-1714, 2006.
- [7] J. Yvonnet., H. Le Quang, Q.-C. He. *An XFEM/level set approach to modelling surface/interface effects and to computing the size-dependent effective properties of nanocomposites*, Comput. Mech., 42, 704-712, 2008.
- [8] J. Yvonnet, A. Mitrushchenkov, G. Chambaud, Q.-C. He. *Finite element model of ionic nanowires with size-dependent mechanical properties determined by ab initio calculations*, Computer Methods in Applied Mechanics and Engineering, 200 :614-625, 2011.